

# Electronic Excited-State Transport in Random Systems. Time-Resolved Fluorescence Depolarization Measurements

C. R. Gochanour and M. D. Fayer\*

Department of Chemistry, Stanford University, Stanford, California 94305 (Received: January 6, 1981;  
In Final Form: February 24, 1981)

Electronic excited-state transport in a system composed of randomly distributed molecules, i.e., rhodamine 6G in glycerol, is experimentally investigated. Time-resolved fluorescence depolarization measurements, which use a fluorescence mixing technique to give subnanosecond time resolution, provide a stringent test for theoretical work on this subject. The results yield an  $R_0$  value of 50 Å for R6G and confirm the results of the recent diagrammatic self-consistent theoretical method. Mean-square displacements and their time derivatives are reported. Energy transport is nondiffusive in the samples studied.

## Introduction

The transport of electronic excited-state energy among a set of identical molecules randomly distributed in a medium such as a solution, glass, or mixed crystal has been a challenging problem for both the theorist and experimentalist for over 30 years. Excited-state transport can lead to processes such as sensitized luminescence and sensitized photochemistry. Forster's original work<sup>1</sup> employed assumptions which led to the description of excited-state transport as inherently diffusive. This provided a qualitative understanding of the transport phenomenon. Very recently the full problem of transport in a random system was attacked<sup>2</sup> and solved.<sup>3</sup> The theoretical results are a quantitative solution to the problem which demonstrate that, in general, transport is not diffusive.<sup>2,3</sup> In this paper a detailed experimental examination of the theory is presented. The experimental results provide strong support for the theory and give the first complete description of electronic excited-state transport in a random system.

The important characteristic of a random system is the statistical distribution of intermolecular distances which leads to a distribution of transfer rates from an initially excited molecule to surrounding unexcited molecules. There is not a single path by which excitation probability is transferred between two molecules but rather an infinite set of possible paths involving all the molecules in the sample. An ensemble average over this set of paths is necessary to describe the actual transfer process. A naturally occurring situation in which it is necessary to perform such an average is in the analysis of the energy-transfer step in the photosynthetic process.

Until recently theoretical work on this problem has been limited to study of very low concentration systems,<sup>2,4,5</sup> i.e., the case in which energy transport is close to negligible. In this situation an excited molecule is taken to interact with a small number of neighboring molecules and is independent of all other molecules in the sample. This approximation is valid when the initial site is the only significant source of excitation probability, i.e., the low-concentration-short-time limit. Examples of such calculations include the steady-state fluorescence depolarization calculations of Craver and Knox,<sup>4</sup> the time-dependent fluorescence depolarization calculation of Hemenger and Pearlstein,<sup>5</sup> and the Green function calculation of Haan and Zwanzig.<sup>2</sup> As will be discussed in more detail below, fluorescence depolarization is related to the probability of

an excitation remaining at the site of initial excitation. The calculations of Craver and Knox<sup>4</sup> and of Pearlstein and Hemenger<sup>5</sup> focus only on this aspect of the problem. The Green function calculation of Haan and Zwanzig<sup>2</sup> although limited to short times or low concentrations contains information concerning the spatial transport of the excited states, e.g., the time-dependent mean-squared displacement, in addition to the initial site probability. Haan and Zwanzig show that transport is nondiffusive in the low-concentration-short-time limit.

As mentioned above, a comprehensive theoretical study of excited-state transport in random systems has been presented recently.<sup>3</sup> This treatment is based on a diagrammatic expansion of the Green function. The technique developed results in an approximate solution which is accurate for all times and concentrations. As this work will be used to analyze the time-dependent fluorescence depolarization data reported in this paper, a summary of the theoretical method and results and the additional details which are necessary to interpret the experimental data are given in section II.

Previously, the most reliable data on excited-state transport in random systems was obtained from concentration-dependent steady-state fluorescence depolarization measurements in viscous solvents.<sup>6</sup> At low concentration, where energy transfer does not occur, the fluorescence polarization reflects the polarization of the excitation source. As the concentration of transfer sites is increased, energy transfer to randomly oriented molecules occurs and the fluorescence is depolarized. The concentration dependence of this effect has been calculated by Craver and Knox,<sup>4</sup> Ore,<sup>7</sup> and others.<sup>5,8</sup> A comparison with experiment has been made by Craver and Knox.<sup>4</sup> Their work indicates agreement which is at least qualitatively good and gives  $R_0$ , the constant which characterizes the strength of the intermolecular transport interactions,<sup>1</sup> for a number of compounds.

A serious drawback of the steady-state method is that measurements on a large number of concentrations span-

(1) Th. Forster, *Ann. Phys. Leipzig*, **2**, 55 (1948).

(2) S. W. Haan and R. Zwanzig, *J. Chem. Phys.*, **68**, 1879 (1978).

(3) C. R. Gochanour, H. C. Andersen, and M. D. Fayer, *J. Chem. Phys.*, **70**, 4254 (1979).

(4) F. W. Craver and R. S. Knox, *Mol. Phys.*, **22**, 385 (1971).

(5) R. P. Hemenger and R. M. Pearlstein, *J. Chem. Phys.*, **59**, 4064 (1972).

(6) A. Kowski, *Z. Naturforsch. A*, **18**, 961 (1963).

(7) A. Ore, *J. Chem. Phys.*, **31**, 442 (1959).

(8) A. Jablonski, *Acta Phys.*, **14**, 295 (1958); G. Weber, *Trans. Faraday Soc.*, **50**, 552 (1954).

\* Alfred P. Sloan Fellow and Dreyfus Foundation Fellow.

ning a wide range of concentrations are necessary in order to make a detailed comparison of theory and experiment. Examination of a wide range of concentrations is experimentally difficult, and the data reported generally consist of measurements on a small number of concentrations.<sup>6</sup> This inhibits comparison of theory and experiment. Furthermore, the theories of fluorescence depolarization, while perhaps capable of confirming the Forster mechanism, do not give the total Green function for the system and are therefore not capable of calculating the transport properties of interest from the experimental results.

In this paper we present the results of time-resolved fluorescence depolarization measurements which permit the study of excited-state transport in random systems in a very precise manner. Using the technique of fluorescence mixing,<sup>9</sup> we are able to measure the time dependence of polarized fluorescence with a time resolution of better than 100 ps. The time-dependent fluorescence depolarization data from a single sample can be employed in a comparison of theory and experiment and provides the value of  $R_0$ . Other concentration samples are then examined experimentally and compared to theory with no adjustable parameters. This provides a stringent test of the theory.

In the experiments presented below, the time-resolved fluorescence depolarization method was used to examine various concentration samples of rhodamine 6G in the viscous solvent glycerol. The agreement between theory and experiment is near perfect.  $R_0$  is 50 Å. The results are used to calculate the mean-square displacement and the time derivative of the mean-square displacement as a function of time and concentration. These measurements confirm the theory and give a detailed description of excited-state transport in this system. They demonstrate that energy transport can be highly nondiffusive in randomly distributed systems.

## Theory

In this section, the theoretical treatment<sup>3</sup> used to describe electronic excited-state transport among molecules distributed randomly in a medium is briefly recounted and the connection to the time-resolved fluorescence depolarization experiment made. This section provides a context in which to discuss the experiments described in sections III and IV.

Each configuration of  $N$  molecules distributed randomly in a volume  $V$  with number density  $\rho$  is characterized by the location and orientation of the  $N$  molecules ( $\bar{r}_1, \Omega_1; \bar{r}_2, \Omega_2; \dots; \bar{r}_N, \Omega_N$ ). The vector  $\bar{r}_i$  gives the location of molecule  $i$  while  $\Omega_i$  represents the set of angular coordinates necessary to specify the orientation of the transition dipole. The master equation for each configuration, denoted by  $R$ , is 
$$dp_j(R, t)/dt = -p_j(R, t)/\tau + \sum_k \omega_{jk} [p_k(R, t) - p_j(R, t)] \quad (1)$$

where  $p_j(R, t)$  is the probability that an excitation is found on molecule  $j$  in configuration  $R$  at time  $t$ ,  $\tau$  is the measured lifetime, and  $\omega_{jk}$  is the transfer rate between molecule  $j$  and  $k$ . For the Forster mechanism  $\omega_{jk}$  is given by

$$\omega_{jk} = \frac{3}{2} \tau^{-1} K_{jk}^2 (R_0/r_{jk})^6 \quad (2)$$

The orientation factor  $K_{jk}^2$  is dependent on the relative orientation of the transition dipoles of molecules  $j$  and  $k$  and can be written as

$$K_{jk}^2 = [\hat{d}_j \cdot \hat{d}_k - 3(\hat{d}_j \cdot \hat{r}_{jk})(\hat{d}_k \cdot \hat{r}_{jk})]^2 \quad (3)$$

where  $\hat{d}_j$  and  $\hat{d}_k$  are unit vectors in the directions of the transition dipoles of molecules  $j$  and  $k$  and  $\hat{r}_{jk}$  is a unit

vector in the direction of a vector connecting molecule  $j$  and  $k$ .

The quantity most useful for obtaining information concerning transport is the Green function, for which the formal solution is

$$G(\bar{r} - \bar{r}', t) = G^s(\bar{r} - \bar{r}', t) + G^m(\bar{r} - \bar{r}', t) \quad (4)$$

where

$$G^s(\bar{r} - \bar{r}', t) = \delta(\bar{r} - \bar{r}') \langle [\exp(t\mathbf{W})]_{11} \rangle \quad (5)$$

$$G^m(\bar{r} - \bar{r}', t) = (N-1) \langle \delta(\bar{r}_{12} - \bar{r} + \bar{r}') [\exp(t\mathbf{W})]_{12} \rangle \quad (6)$$

The brackets denote and ensemble average over possible configurations<sup>10</sup>

$$\langle F(R) \rangle = [1/(4\pi V)]^N \int d\bar{r}_1 \int d\Omega_1 \dots \int d\bar{r}_N \int d\Omega_N F(R) \quad (7)$$

and the matrix  $\mathbf{W}$  is defined by

$$W_{jk} = \omega_{jk} - \delta_{jk} \sum_i \omega_{ji} \quad (8)$$

The Green function can be thought of as the probability of finding an excitation at position  $\bar{r}$  and time  $t$  with the initial condition of unit probability at  $\bar{r}'$ . It is convenient to divide the Green function into two terms, one which is a measure of probability at the initial site of excitation  $\bar{r}'$ ,  $G^s(\bar{r} - \bar{r}', t)$ , and one which is a measure of the probability found on a molecule a distance  $\bar{r} - \bar{r}'$  from the initial site,  $G^m(\bar{r} - \bar{r}', t)$ .

The two components of the Green function can be expanded in diagrammatic series. To do this it is convenient to work with the Fourier-Laplace transforms of  $G^s(\bar{r} - \bar{r}', t)$  and  $G^m(\bar{r} - \bar{r}', t)$ ,  $\hat{G}^s(\epsilon)$  and  $\hat{G}^m(\bar{k}, \epsilon)$ .  $\hat{G}^s(\epsilon)$  and  $\hat{G}^m(\bar{k}, \epsilon)$  are given by

$$\hat{G}^s(\epsilon) = \langle [(\epsilon - \mathbf{W})^{-1}]_{11} \rangle \quad (9)$$

$$\hat{G}^m(\bar{k}, \epsilon) = (N-1) \langle \exp(i\bar{k} \cdot \bar{r}_{12}) [(\epsilon - \mathbf{W})^{-1}]_{12} \rangle \quad (10)$$

The diagrammatic series corresponding to each of these functions is obtained by expanding the matrix  $(\epsilon - \mathbf{W})^{-1}$  in powers of  $\epsilon$  and  $\mathbf{W}$ . After substituting the definition of  $W_{jk}$  into this series an infinite series of products of  $\omega_{jk}$  factors results. Each of these products is then associated with a diagram. The complexity of the diagrammatic series can be decreased through a topological reduction. This procedure involves examination of the topological structure of the  $\hat{G}^m(\bar{k}, \epsilon)$  diagrammatic series to find a smaller set of  $\hat{G}^m(\bar{k}, \epsilon)$  diagrams from which all diagrams can be generated. The resulting series of diagrams, the  $\hat{\Sigma}(\bar{k}, \hat{G}^s(\epsilon))$  series, is both a function of  $\hat{G}^s(\epsilon)$  and can be used to generate  $\hat{G}^s(\epsilon)$ . This self-consistency property is used to generate an approximate solution for the Green function.

The results of the diagrammatic method reproduce analytically the low-concentration-short-time results of Haan and Zwanzig.<sup>2</sup> In addition, the calculations yield infor-

(10) In ref 3, the theory is developed by use of the orientation-averaged Forster rate. Thus the configuration averages used to calculate the Green function did not include an orientation average. This method was chosen to simplify the theoretical development. In this work we properly account for the orientation factor by calculating the orientation-averaged Green function explicitly. For the first approximation ("two-body") the orientation average can be performed exactly. The form obtained for  $G^s(t)$  is identical with that obtained with the orientation-averaged rate with a replacement of  $C$  by  $\gamma C$ . The angular integrations needed to obtain the second approximation ("three-body") are much more difficult and have not been calculated exactly. We have assumed that the effect of the angular averages in the three-body terms is the same as in the two-body terms, i.e.,  $C$  is replaced by  $\gamma C$ . As the three-body corrections to the two-body approximation are small, the errors in this approximation will not affect the results presented here. Similar approximations have been used to obtain eq 11.

mation on the system's intermediate and long-time behavior. The results show that, for all concentrations, excited-state transport becomes diffusive at sufficiently long times. The long-time diffusion constant is given by

$$D = 0.374C^{4/3}R_0^2\tau^{-1} \quad (11)$$

For low concentration systems, transport becomes diffusive only at very long times, i.e., after more than a few lifetimes, and thus for all practical purposes transport is not diffusive. For high concentrations transport becomes diffusive within one lifetime.

If a solution of molecules in a viscous solvent is irradiated with a short pulse of polarized light, molecules with their transition dipoles oriented parallel to the excitation polarization are preferentially excited. If the ensuing fluorescence is detected through a polarizer, the initial ratio of parallel polarized fluorescence intensity to perpendicular polarized intensity is 3:1. In a low concentration sample where energy transfer does not occur, both components of the fluorescence decay with the lifetime and the polarization ratio is preserved. In higher concentration samples excited-state population is transferred among randomly oriented molecules and the fluorescence is depolarized. Galanin has shown that the overwhelming contribution to fluorescence polarization is due to fluorescence from excitations at sites which were initially excited,<sup>4,11</sup> i.e., energy transfer can be assumed to occur to a randomly oriented molecule. Thus the time dependence of fluorescence depolarization will be related to the time-dependent probability that the excitation is at the initial site. For the theoretical model we have derived, this probability is given by the inverse Laplace transform of  $\hat{G}^s(\epsilon)$ , which will be denoted by  $G_s(t)$ .  $\hat{G}^s(\epsilon)$  is given by

$$\hat{G}^s(\epsilon) = \tau\{(\pi^2\gamma^2C^2/4)[1 - [1 + (32/\pi^2\gamma^2C^2)(\epsilon\tau - 0.1887\gamma^2C^2)]^{1/2}] + 4(\epsilon\tau - 0.1887\gamma^2C^2)\}/[4(\epsilon\tau - 0.1887\gamma^2C^2)^2] \quad (12)$$

where the unitless concentration  $C$  is given by

$$C = \frac{4}{3}\pi R_0^3\rho \quad (13)$$

$$\gamma = 0.846 \quad (14)$$

$G^s(t)$  is obtained from eq 12 by numerical inversion of the Laplace transform.<sup>12</sup>

Thus the fluorescence arises from two ensembles. The first, with a weighting factor  $G^s(t)$ , consists of molecules initially excited and the resulting fluorescence is polarized. The second ensemble, with a weighting factor  $(1 - G^s(t))$ , consists of molecules to which excited-state energy has been transferred; the fluorescence from these sites is unpolarized. Calculation of the component of the fluorescence with a given polarization for each of these ensembles is straightforward. The following results are obtained

$$I_{\parallel}(t) = e^{-t/\tau}(1 + 0.8G^s(t)) \quad (15a)$$

$$I_{\perp}(t) = e^{-t/\tau}(1 - 0.4G^s(t)) \quad (15b)$$

where  $I_{\parallel}$  is the fluorescence intensity polarized parallel to the excitation polarization and  $I_{\perp}$  is the fluorescence intensity polarized perpendicular to the excitation polariza-

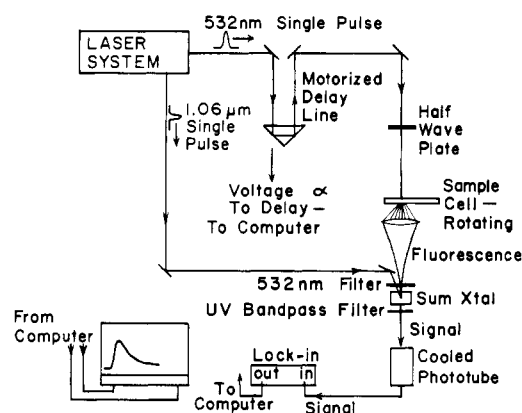


**Figure 1.** Time-resolved fluorescence depolarization experimental setup. The laser system consists of a high-repetition-rate mode-locked Nd:YAG laser with the necessary accessories to yield picosecond time scale single pulses at 1.06  $\mu\text{m}$  and 532 nm. The sample is excited with the 532-nm pulse. The resulting fluorescence is mixed with the 1.06- $\mu\text{m}$  pulse to produce a short pulse of UV light. This mixing technique provides time resolution. A half-wave plate is used to change the polarization of the excitation pulse relative to the polarization of the detection pulse.

tion. Equations 15a and 15b show the direct path from the experimental observables to the system's Green function and thus to a detailed description of the excited-state transport.

## Experimental Section

The time-resolved fluorescence depolarization measurements were made by using the fluorescence mixing method<sup>9</sup> illustrated schematically in Figure 1. The laser is a continuously pumped acoustooptically Q-switched and mode-locked Nd:YAG laser built in house and modeled on a device developed at Stanford.<sup>13</sup> The 1.06- $\mu\text{m}$  single-pulse output is frequency doubled and the resulting beam spatially separated into 1.06- $\mu\text{m}$  and 532-nm components. The green single pulse is used to excite the sample. The resulting fluorescence is filtered to remove scattered green light and focused into a KDP type-II sum-generating crystal where it overlaps with the path of the 1.06- $\mu\text{m}$  single pulse. The fluorescence reaching the sum crystal coincident in time with the 1.06- $\mu\text{m}$  pulse mixes with the 1.06- $\mu\text{m}$  pulse to produce a short burst of UV light (390 nm). The UV intensity is proportional to the fluorescence intensity at that time. The sum crystal is oriented so that only the component of the fluorescence polarized perpendicular to the 1.06- $\mu\text{m}$  polarization sums. When a half-wave plate is used, the polarization of the excitation pulse is varied relative to the 1.06- $\mu\text{m}$  pulse. This permits examination of  $I_{\parallel}$  and  $I_{\perp}$ .

The time decay is swept out by varying the delay between the green excitation pulse and the 1.06- $\mu\text{m}$  detection pulse with a motorized delay line. The signal is observed through a UV bandpass filter by a cooled photomultiplier (EMI 6256). The phototube output is measured with a lock-in amplifier set at the laser frequency. The output of the lock-in and a voltage proportional to the delay time are converted to digital form and stored on disk by using a minicomputer. The digital data storage facilitated the data analysis presented in the next section.

The samples consisted of known concentrations of rhodamine 6G (New England Nuclear, Pilot No. 559) dissolved in glycerol. The solution is placed in a rotating sample cell of approximately 7.5 cm diameter formed by

(11) Galanin has shown that the polarization retained is very small, assuming a random distribution of dipole orientations for the acceptor molecules. In the experiments described here the fraction of molecules excited is small so this assumption is valid as demonstrated by the lack of a power dependence of the signal at the energy densities utilized in these experiments. M. D. Galanin, *Tr. Fiz. Inst. I. P. Pavlova*, 5, 341 (1950).

(12) H. Stehfest, *Commun. Assoc. Comput. Mach.*, 13, 47, 624 (1970).

(13) D. J. Kuizenga, D. W. Phillion, T. Lund, and A. E. Siegman, *Opt. Commun.*, 9, 221 (1973).

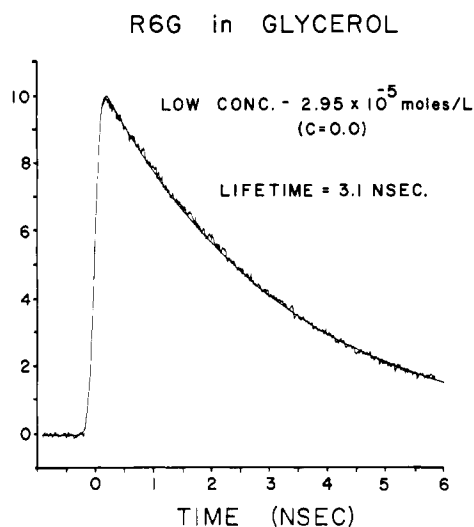


**Figure 2.** Time-resolved fluorescence depolarization data for a very low concentration sample ( $2.95 \times 10^{-5}$  mol/L) of R6G in glycerol. At this low concentration excited-state transport does not occur, i.e., the Forster reduced concentration is  $C = 0.0$ . The data are identical for the parallel and perpendicular polarizations. These data yield a lifetime  $\tau = 3.1$  ns and demonstrate that rotational depolarization does not occur and that the data are free from experimental artifacts.

two glass flats separated by thin foil spacers. The sample cell is rotated to avoid effects due to photodecomposition or heating. The cell thickness was adjusted from 300 to 5  $\mu\text{m}$  to control the optical density of the various concentration samples in order to eliminate reabsorption problems.

### Results and Discussion

The excitation and detection pulses have finite duration, therefore eq 15a and 15b must be convolved with the pulse shapes to obtain theoretical curves which can be compared with experimental data. Autocorrelation and cross correlation measurements indicate that both excitation and detection pulses are Gaussian with pulse durations (fwhm) of 100 and 140 ps, respectively. Thus the convolution integrals are of the form

$$S(t_D) = \int_{-\infty}^{+\infty} dt \exp[-4(\ln 2) \times (t - t_D)^2 / W_1^2] \int_{-\infty}^t dt' \exp[-4(\ln 2)t'^2 / W_2^2] H(t - t') \quad (16)$$

where  $S(t_D)$  is the observed signal at time delay  $t_D$ ,  $W_1$  and  $W_2$  are the detection and excitation pulse durations (fwhm) respectively, and  $H(t - t')$  is the impulse response function. The convolutions are calculated numerically by using the appropriate form for the impulse response function, eq 15a or 15b.

In Figure 2 the parallel component of the time-resolved fluorescence depolarization data is shown for a sample of concentration  $2.95 \times 10^{-5}$  mol/L. This sample corresponds to the  $C = 0.0$  limit, i.e., excited-state transport is negligible. The decays of both parallel and perpendicular components of the fluorescence are identical. They decay exponentially with a lifetime of  $3.1 \pm 0.1$  ns. In addition to providing the lifetime which is a necessary input for the theory, the low concentration data demonstrated that molecular rotation is much slower than the lifetime and thus depolarization effects due to molecular rotation<sup>14</sup> do

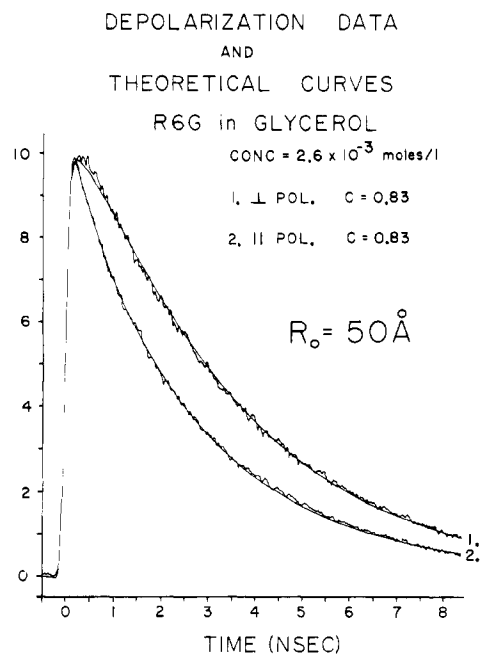


**Figure 3.** Depolarization data and theoretical curves for a sample of R6G in glycerol of concentration  $2.6 \times 10^{-3}$  mol/L. The decay of the parallel component is faster than the lifetime decay and the decay of the perpendicular component slower than the lifetime decay due to excited-state transport-induced depolarization. A single parameter fit yields  $R_0 = 50$  Å. The functional form of the theoretical curves show excellent agreement with the data.

not occur on the time scale of the experiment. Furthermore, the excellent agreement between the experimental data and the curve calculated by using eq 16 demonstrates that the data are free of artifacts and that the convolutions can be handled accurately.

For higher concentrations samples it is possible to extract the lifetime by measuring the decay of the component of the fluorescence with a polarization  $54^\circ 44'$  from the excitation polarization ("magic angle"). At the magic angle, depolarization effects vanish and the time dependence of the total excited-state population is measured. Such measurements were used to ensure that reabsorption (radiative transfer) did not affect the depolarization data reported here. At the highest concentration studied the observed lifetime was somewhat faster than the low concentration value of 3.1 ns.<sup>15</sup> For this concentration ( $5.3 \times 10^{-3}$  mol/L) the decrease in the lifetime was small,  $\sim 250$  ps, and the difference could be corrected for by using the observed lifetime in eq 15a and 15b.

The effect of increasing concentration can be seen in the data in Figure 3. For a concentration of  $2.6 \times 10^{-3}$  mol/L the decay of the parallel component of the fluorescence is found to be faster than the 3.1-ns exponential decay obtained at low concentration while the decay of the perpendicular component is slightly slower than the lifetime decay. Both data sets show excellent agreement with the theoretical curves (solid line) calculated by using eq 15a and 16 with  $\tau = 3.1$  ns and adjusting the reduced concentration to  $C = 0.83$ . When this value of  $C$  is used and the concentration is in mol/L, a value of 50 Å is obtained for  $R_0$ . By varying the reduced concentration and comparing the fit obtained we found it possible to place

(15) The observed decrease in lifetime at high concentration is due to trapping on loosely bound dimer complexes which have a short lifetime. At very high concentrations this effect dominates the observed lifetime decay. A detailed study is in preparation (ref 16).

(16) D. Lutz, K. Nelson, M. Fayer, and C. Gochanour, to be published.

(14) T. J. Chuang and K. B. Eisenthal, *Chem. Phys. Lett.*, 11, 368 (1971).

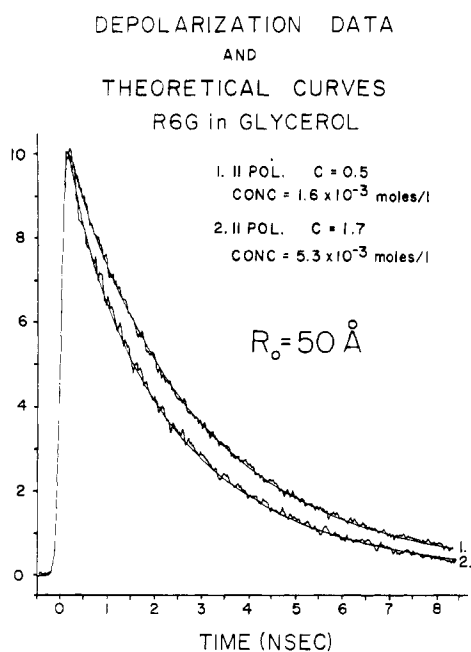


**Figure 4.** Depolarization data and theoretical curves for the parallel component of the fluorescence for concentrations corresponding to  $C = 0.5$  and  $C = 1.7$ . When the measured lifetime and  $R_0 = 50 \text{ \AA}$  were used the theoretical curves for these concentrations were calculated with *no adjustable parameters*. The agreement between theory and experiment is near perfect. The same quality of agreement was obtained for a variety of sample concentrations. These results confirm the diagrammatic self-consistent theoretical method and yield a comprehensive description of excited-state transport.

an error bar of approximately  $\pm 2 \text{ \AA}$  on this value for  $R_0$ .

With  $\tau$  and this value of  $R_0$  it is now possible to calculate the time-dependent signal for any concentration sample with *no adjustable parameters*. Several concentrations were studied in this manner. In Figure 4, the decay of the parallel component of the fluorescence is shown for solutions having reduced concentrations of  $C = 0.5$  and  $C = 1.7$ . The solid lines through the data are the theoretical curves calculated for these concentrations. The agreement between the experimental data and the no adjustable parameter theoretical curves is near perfect for both concentrations. Similar agreement has been obtained for the decay of the perpendicular component of the fluorescence decay.

As discussed earlier, the theoretical method we have results in an excellent approximation to the full Green function. If the approximation and the experimental results reported here are used it is possible to calculate the transport properties of the system studied. In Figures 5 and 6 the mean-square displacement and its time derivative are displayed for  $C = 0.5$  and  $C = 1.7$ , and for  $C = 5.0$ . To emphasize the transport properties of the system, we calculated the figures without the exponential decay due to the lifetime. Thus in Figure 5, the mean-square displacement at time  $t$  is for the ensemble of excited states present at  $t$ . (The fraction of the initially excited population remaining at  $t$  is obtained by evaluating  $\exp[-t/\tau]$ .) From Figure 6 it can be seen that for  $C = 0.5$ , transport is nondiffusive over the entire time range studied. This is also true for  $C = 1.7$ , although it is approaching the diffusion limit by  $t = 2\tau$ . For higher concentrations, the diffusive limit is reached within one lifetime as can be seen from the  $C = 5.0$  curve. The mean-square displacement curves yield interesting information concerning the transport of the excitation. For  $C = 1.7$  and  $t = \tau$ , the root-mean-square displacement is  $117 \text{ \AA}$ . This corresponds

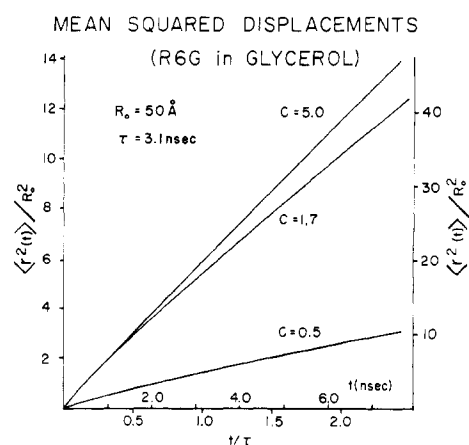


**Figure 5.** Theoretically calculated time-dependent mean-square displacements for several concentrations of R6G in glycerol. These were calculated by using the experimental parameters obtained here and the diagrammatic self-consistent theoretical method.<sup>3</sup> The excited-state lifetime has been removed to show more clearly the time-dependent nature of the transport properties (see text). The left scale is for the two low concentration curves and the right scale applies to the highest concentration curve only.

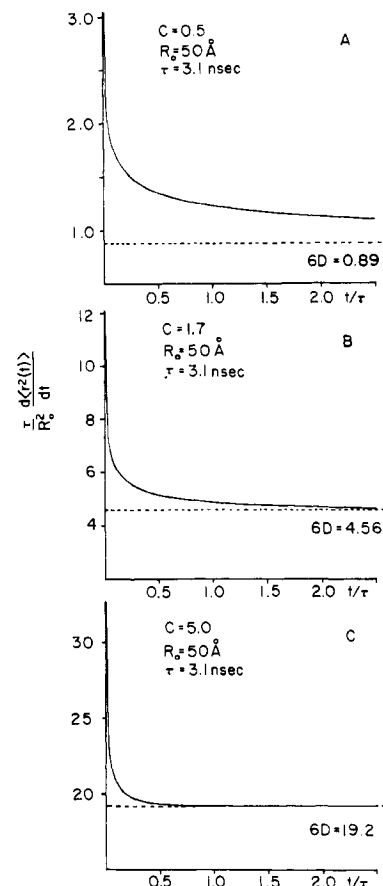


**Figure 6.** Calculated time derivatives of the mean-square displacements given in Figure 5. The dashed lines indicate the theoretical value of the long time limit diffusion rate. For  $C = 0.5$  (Figure 6A) transport is not diffusive during the first several lifetimes. For  $C = 1.7$  (Figure 6B) transport is approaching the diffusive limit by two lifetimes. For  $C = 5.0$  (Figure 6C) transport becomes diffusive within one excited-state lifetime.

to a volume in which the average number of molecules is about 21. For  $t = 2\tau$  the excitation is distributed over a volume in which the average number of molecules is 50. Even for this relatively low concentration, it is clear that theoretical treatments which include only interactions

among 2 or 3 near neighbors are inadequate to describe the transport properties of a random system over full ranges of time and concentration.

The spectral overlap method developed by Forster<sup>1</sup> and used by Kawski<sup>6</sup> yields a value of 47 Å for  $R_0$ . As this determination requires a difficult measurement of the absorption and fluorescence lineshapes, it is probably within experimental error of the value reported here. These measurements have recently been carefully repeated and yield a value of  $R_0$  of 50 Å with an error bar of less than 1 Å.<sup>17</sup> Thus in this system accurate spectroscopic measurements combined with the proper theoretical treatment can be used to calculate the dynamics of energy transfer. A number of similar liquid solution systems are presently under investigation, using both spectroscopic and time-dependent methods to determine the general applicability of the spectroscopic approach. Other types of materials are also under investigation. Holstein, Lyo, and Orbach have pointed out that the spectroscopic method may be of limited value in certain types of systems.<sup>18</sup> In many systems direct time-dependent measurements are necessary.

### Concluding Remarks

In this paper we have presented experimental data on excited-state energy transport in random systems. By observing the time-resolved fluorescence depolarization on a subnanosecond time scale using a fluorescence mixing

technique we are able to obtain data which provide a stringent test of the diagrammatic self-consistent theoretical method. Owing to the time-resolved nature of the experiments, each experimental sample provides detailed information on excited-state transport. By examining several samples of different concentrations, we found it possible to test the theory with no adjustable parameters.

The experimental results confirm the theoretical description and demonstrate that excited-state transport can be highly nondiffusive in random systems. At short times, transport is considerably faster than transport would be if it were governed at all times by the long-time-limit diffusion constant. Assuming diffusive transport can lead to an overestimation of the strength of intermolecular transport interactions. It is important to realize that the nondiffusive behavior manifested in the theory does not result from any type of "coherence" effects but rather from a detailed examination of this strictly "incoherent" physical situation.

We are in the process of studying a variety of other experimental systems. Although the theory and experiments presented here were applied to solutions, the theoretical method can be applied to other types of materials. Finally, it is anticipated that a detailed understanding of random systems will give us the ability to examine systems of unknown structure, e.g., photosynthetic units, with an eye toward understanding excited-state transport and obtaining detailed structural information.

*Acknowledgment.* This work was supported by the Department of Energy, Division of Materials Research under Contract DE-AT03-79ER 10467.

(17) M. Ediger and R. Moog, private communication.

(18) T. Holstein, S. K. Lyo, and R. Orbach, *Phys. Rev. Lett.*, **36**, 891 (1976).

## A Test of the Isolated Binary Collision Model: Relaxation of Vibrationally Excited Carbon Monoxide by Oxygen in Liquid Argon<sup>†</sup>

David W. Chandler<sup>‡</sup> and George E. Ewing\*

Department of Chemistry, Indiana University, Bloomington, Indiana 47405 (Received: January 16, 1981; In Final Form: March 24, 1981)

We have measured the vibrational relaxation of CO\* by O<sub>2</sub> dissolved in liquid Ar by monitoring its infrared fluorescence. The relaxation rate constant for the liquid-phase system is *lower* than for the gas-phase system. The isolated binary collision (IBC) model predicts a *higher* rate constant in the liquid phase. The model is examined and possible explanations for the discrepancy are presented. However, if one considers the simplicity of the IBC model and that its predictions differ from the observations by less than an order of magnitude it remains a valuable guide to liquid-state vibrational relaxation processes.

### Introduction

Is the isolated binary collision (IBC) model useful for explaining vibrational relaxation processes in liquids? This model, originally proposed by Litovitz,<sup>1</sup> says that the relaxation rate of a vibrationally excited molecule in the liquid state is faster than in the gaseous state only because the density is higher and there are more binary collisions. Various recipes have been offered for calculating the collision frequency as a function of the density of the

phase. A number of theoretical studies have critically examined the assumptions and applicability of the IBC model.<sup>2-4</sup> For all the discussion, the IBC model has great appeal because of the simplicity of its concept and the ease with which it may be applied. But, how well does it work?

Several experimental studies have shown, for a range of temperatures and densities in the gas and liquid phase, that the IBC model does indeed work. Early measure-

<sup>†</sup>Contribution No. 3388 from the Chemical Laboratories of Indiana University.

<sup>‡</sup>Stanford University, Department of Chemistry, Stanford, CA 94305.

(1) T. A. Litovitz, *J. Acoust. Soc. Am.*, **26**, 469 (1956).

(2) W. M. Madigosky and T. A. Litovitz, *J. Chem. Phys.*, **34**, 489 (1961).

(3) P. K. Davis and I. Oppenheim, *J. Chem. Phys.*, **57**, 505 (1972).

(4) D. W. Oxtoby, *Adv. Chem. Phys.*, to be published.